# Nanoscale

Accepted Manuscript


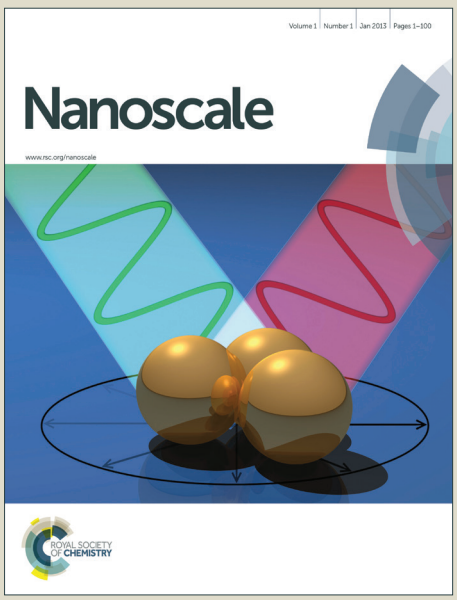





ROYAL SOCIETY OF CHEMISTRY

www.rsc.org/nanoscale

Nanoscale

RSCPublishing

ARTICLE

# Single-digit-resolution nanopatterning with extreme ultraviolet light for the 2.5 nm technology node and beyond†

Cite this: DOI: 10.1039/x0xx00000x

N. Mojarad,[a††*] M. Hojeij,[b††] L. Wang,[c] J. Gobrecht[a] and Y. Ekinci[a*]

Received ooth January 2012,
Accepted ooth January 2012

DOI: 10.1039/x0xx00000x

www.rsc.org/

All nanofabrication methods come with an intrinsic resolution limit, set by their governing physical principles and instrumentation. In the case of extreme ultraviolet (EUV) lithography at 13.5 nm wavelength, this limit is set by light diffraction and is ≈3.5 nm. In the semiconductor industry, the feasibility of reaching this limit is not only a key factor for current developments of lithography technologies, but is also an important factor in deciding whether photon-based lithography will be used for future high-volume manufacturing. Using EUV-interference lithography we show patterning with 7 nm resolution in making dense periodic line-space structures with 14 nm periodicity. Achieving such cutting-edge resolution has been possible by integrating a high-quality synchrotron beam, precise nanofabrication of masks, very stable exposure instrumentations, and utilizing effective photoresists. We have carried out our exposures on silicon- and hafnium-based photoresists and we demonstrated the extraordinary capability of the later resist to be used as a hard mask for pattern transfer into Si. Our results confirm the capability of EUV lithography in the reproducible fabrication of dense patterns with single-digit resolution. Moreover, it shows the capability of interference lithography using transmission gratings in evaluating the resolution limits of photoresists.

## Introduction

The semiconductor industry has continuously evolved in making more compact, efficient, and faster integrated circuits (ICs) with lower costs, predicted by Moore's law[1]. This trend has been the industry's roadmap for around five decades and enabled with steady downscaling of feature sizes through the advancement of lithographic techniques[2]. Optical lithography has been the dominant patterning method due to its high resolution and throughput capability. In optical lithography the resolution ($R$) scales linearly with the illumination wavelength ($\lambda$), and as a result, the wavelength used for high-volume manufacturing (HVM) has over decades reduced in steps from visible, to currently used deep ultraviolet (DUV) immersion lithography at $\lambda$=193 nm for the 22 nm technology node[2]. This small dimension is beyond the resolution capability of DUV lithography and has been achieved thanks to double patterning techniques. Further reduction of $R$ using this technology is accompanied with increasing costs and faces sever physical limitations[3]. As for the next step, lithography at extreme ultraviolet (EUV) wavelength of $\lambda$=13.5 nm (92 eV) was proposed several years ago[4], and after enormous academic and industrial developments, is taking its final steps to enter HVM[3]. The choice of using EUV light for next generation lithography was based on many advantages it provides. First, this wavelength is short enough to reach sub-10 nm imaging resolutions set by light diffraction. Moreover, high-power sources and efficient reflective optics operating at this wavelength could be developed[1, 2]. On the material side, optical absorption at this wavelength is generally very high, allowing for developing efficient photoresists. Besides, exposure at this short wavelength also significantly reduces the proximity effect, while in comparison to soft X-ray lithography, it does not suffer from high scattering and blur caused by long mean-free-path of the secondary electrons[5]. The demanding and expensive transition from DUV to EUV has involved many difficulties such as all-in-vacuum operation, different photochemistry, light source, and efficient optics, to name a few. Therefore, the stimulating question that has been addressed by different parties of the EUV lithography (EUVL) community is that to what extend can the patterning resolution be improved using such wavelength, and could it be effectively used for single-digit patterning? Although reports have shown using different top-down and bottom-up methods for making sub-10-nm features[6-13], none could satisfy stringent RLS specifications, that is, resolution, line-edge roughness (LER), and sensitivity (S), in the extent that EUVL can. On the other hand, the speculation of optical lithography satisfying these

criteria brought non-photon-based options on the table such as highly parallel electron-beam lithography (EBL)[14-16], nanoimprint lithography[17, 18] , and using block copolymers[19-21]. The aforementioned question on the ultimate limitation of EUVL has been a matter of intensive investigation and limiting effects, such as photon-shot noise, secondary electron blur, and feasibility of high-NA optics, have been studied[22]. In this regard, demonstrating the ultimate resolution of EUVL is of strategic importance, since it is part of the puzzle to answer questions on to what extent photon-based lithography can be used for reaching future technology nodes.

We have used EUV interference lithography (EUV-IL) at the Swiss Light Source synchrotron facility to pattern photoresists with highest optical resolutions. We have studied hydrogen silsesquioxane (HSQ) and a novel hafnium-based photoresist, Inpria XE15IB (IB), and have shown their performance in providing dense periodic structures with sub-10 nm half-pitch (HP). Reaching such high performances has been possible thanks to the unique chemical compositions of the resists, the high quality of the illumination and diffraction optics, and the mechanical stability of the exposure instrumentation. The capability of making such dense periodic arrays matches the criteria of the International Technology Roadmap for Semiconductors (ITRS) for reaching the 2.5 nm technology node and beyond[23].

## Results

The general schematic of EUV-IL for making line-space patterns is illustrated in Fig. 1a, where the coherent synchrotron beam is diffracted by a set of two parallel gratings. These two beams interfere at a certain distance from the mask and form a sinusoidal aerial image. This relatively simple method enables making periodic[24] and quasiperiodic[25] nanostructures and evaluating the RLS performance of various photoresists with resolution capabilities beyond the tools using projection optics[26, 27]. Fig. 1b shows scanning electron micrographs (SEMs) of successful patterning of line-space structures with HP in the range of HP=8—11 nm on both photoresists, which are uniform over the designed area of ~100×100 μm$^2$. In terms

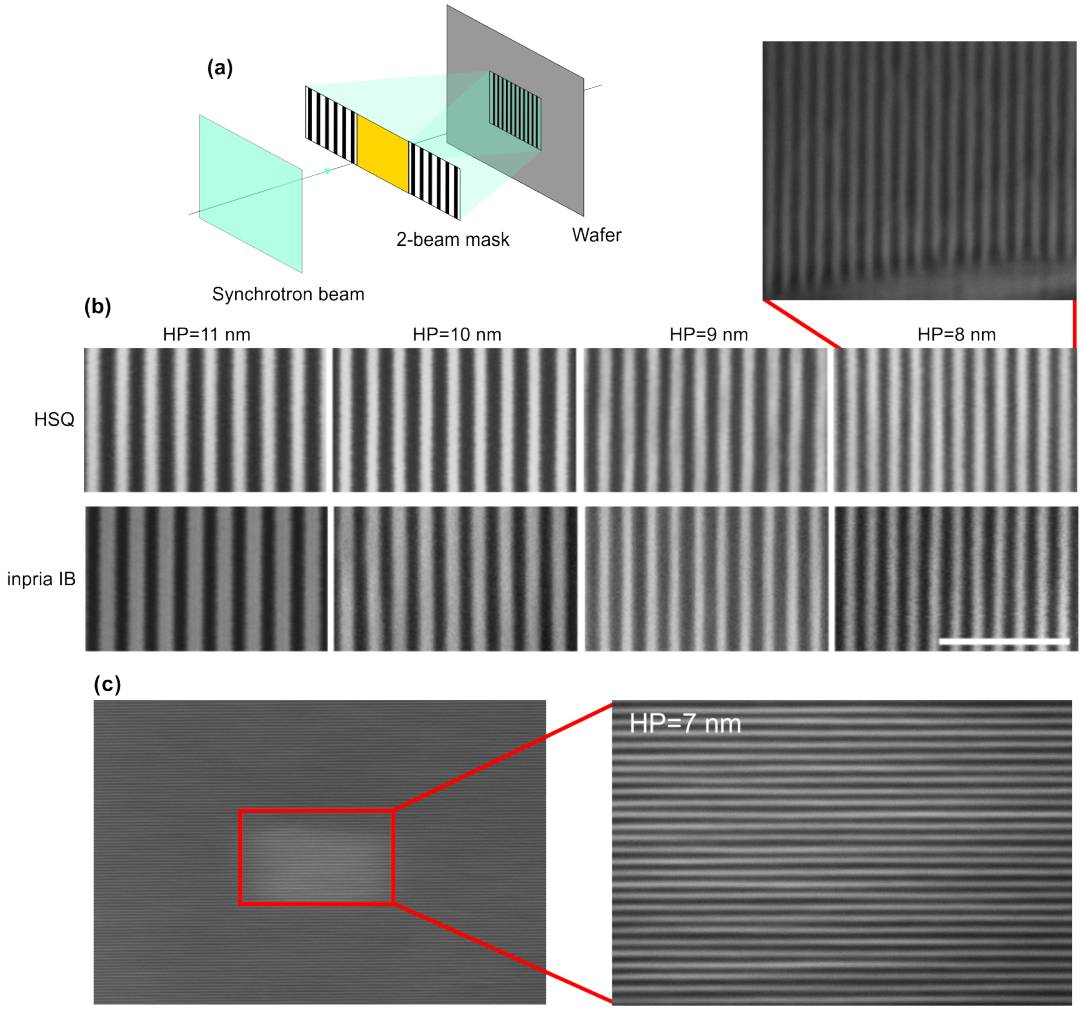


**Fig. 1** High-resolution interference lithography for patterning line-space structures. (a) Schematic of the interference lithography setup for fabricating line-space patterns. (b) Scanning-electron micrographs of line-space gratings with different half pitches (HPs) made by EUV interference lithography on HSQ (top row) and Inpria IB (bottom row). The scale bar is 100 nm. The top right image shows bird-eye view (60° tilt) of HSQ structures with HP=8 nm. (c) A ~2x1.5 μm$^2$ area of uniformly patterned HSQ structures with HP=7 nm and a zoomed image of the indicated area.



 

of resolution, HSQ shows a better performance and, as shown in Fig. 1c, we were also able to obtain HP=7 nm structures. The height of these structures was about 20 nm for both photoresists and they revealed no collapse, bridging or pinching over their entire field. The used IL transmission mask holds a series of parallel gratings with different periodicity and, as a result, all these structures with different HP values were illuminated under the same conditions and in the same exposure. To the best of our knowledge, this is the highest resolution that has been achieved using optical lithography and promises the possibility of reaching sub-2.5 nm technology nodes. The foundation of achieving this resolution is based on successful integration of several main elements: high-performance photoresists, mask-fabrication technology, stable source and interferometer, each being explained in following sections.

Both photoresists are negative tone, non-chemically amplified, and inorganic but have different backbone chemistries. The interaction of HSQ with high-energy electrons and photons has been well studied and it has shown supreme resolutions[28, 29]. The chemistry behind this performance can be briefly described as follows: HSQ molecules are monomers in a cage form of $(HSiO_{3/2})_{2n}$ with different sizes. During the exposure SiH bonds, that are weaker than SiO bonds, are broken and form silanol groups (Si–OH) in the presence of moisture. Since these groups are unstable, they condense to break the caged and form a linear network, which is insoluble in alkaline solution, such as tetramethyl ammonium hydroxide (TMAH) or a base such as NaOH in buffer solution (We used Microposit 351 from Rohm and Haas for our experiments). Inpria IB is an aqueous and hafnium-based resist[30], where the high-energy photons and electrons interact with Hf-bound peroxo ligands, where the O−O bond of the peroxo group dissociate and open hafnium oxo clusters for condensation reactions and reduce solubility in TMAH. Unlike organic photoresists such as PMMA the building blocks of our studied high volume-density inorganic photoresist have sub-nm dimensions and do not consist of polymer chains with large radius of gyration[31]. Moreover, in comparison to chemically-amplified resists (CARs), the reactions in our studied materials are very localized, i.e. there is no acid-diffusion blur. Consequently, these photoresists show such high-resolution performance and reveal smooth edges (i.e. low LER).

For cost-effective utilization of a photoresist, beside the resolution it provides, it is also important that the exposures are done in the shortest possible time. The sensitivity of the two photoresists to EUV illumination was studied by carrying out dose-to-clear exposures. In this process a thin layer of spin-coated photoresist (≈25 nm) is exposed through an open frame at different dose values, $D$. After development, the photoresist height is mapped as a function of $D$, and the 50% clearance of the fitted dose response function, $D_0$, is regarded as the sensitivity[26]. Fig. 2 illustrates these curves, and as it can be seen for the Inpria resist $D_0$=45.5 mJ/cm$^2$, that is, ~7 times more sensitive than HSQ with $D_0$=314.4 mJ/cm$^2$. This significantly higher sensitivity is mainly attributed to the higher atomic absorptions of Hf in the Inpria resist in comparison to Si in

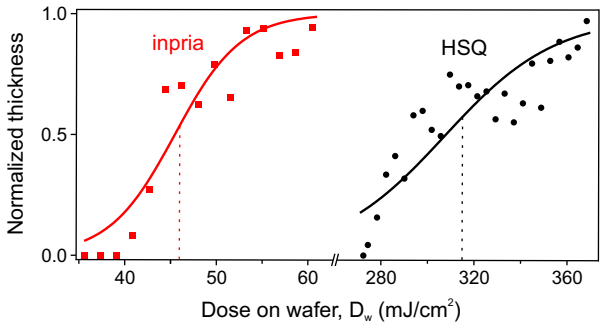


**Fig. 2** Dose-to-clear measurements. Normalized measured photoresist thickness and fitted contrast curves of Inpira IB (red) and HSQ (black) under EUV exposure. The dashed lines indicate the 50% clearance dose.

HSQ's chemical composition. Theoretical calculations of the linear attenuation length, $l$, indicate that under EUV illumination for hafnium $l_{Hf}$=31 nm, while for silicon $l_{Si}$=588 nm[32]. Inpria IB is clearly advantageous by providing similar resolution with much higher sensitivity.

The dose-to-size, i.e. average dose of aerial image to obtained 1:1 line-spaces, for Inpria IB is in the range of 200-250 mJ/cm$^2$ (Fig. S3 in supplementary information). This dose is relatively independent of the HP due to the pitch-independent contrast of IL, a general observation for all resists. We would like to point out that HSQ could also be patterned with ~1/3 of this dose by developing with TMAH instead of 351. However, patterns made with this procedure do not show clean features for HP<10 nm. It should be noted that the sensitivity of Inpria IB is around one order of magnitude lower than the most advanced CARs[26], while such CARs can only provide down to HP=16 nm with low LER. The SEM imaging recipes had to be modified for best visualization of the resolution in Fig. 1, due to the very thin and high resolution resist patterns. Still, with the current resolution we reach the limitations of the imaging and therefore were not able to obtain quantitative LER values. A reliable quantitative evaluation can only be made using more advanced tools such as transmission-electron microscopy.

Grating-based IL has several advantages that allow us to

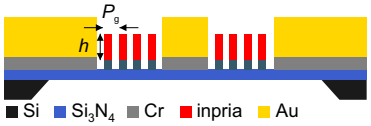


**Fig. 3** Schematic of the high-resolution transmission-grating mask.

carry out nanolithography with single-digit resolution. It has no projection optics and therefore the resolution is not limited by the numerical aperture (NA) and no imaging aberration is transferred into the aerial image. Moreover, it has no depth of focus, and as a result there is no contrast loss due to being out of focus. These advantages are particularly important at the EUV wavelength. Another advantage of EUV-IL is its achromatic nature where:

$$HP=P_g/4m, \quad (1)$$

with $m$ being the diffraction order and $P_g$ the on-mask grating pitch (this relation holds true for two-beam IL). According to

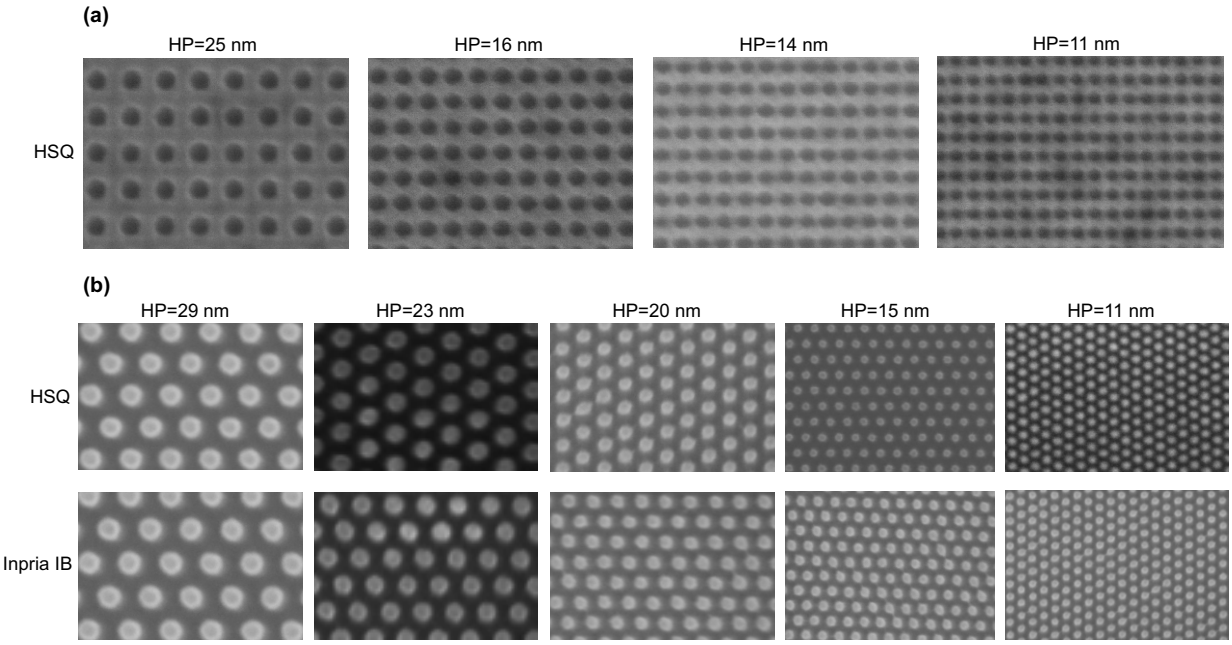


**Fig. 4** SEMs of two-dimensional arrays with different periodicities. (a) Hole array with rectangular lattice, patterned on HSQ. (b) Dot array with triangular lattice, patterned on HSQ (top row) and Inpria IB (bottom row).

Eq. 1 EUV-IL enables frequency multiplication of the grating structure on mask at least by a factor of two using $m$=1 diffracted beams. The results presented in this article are also obtained by the interference of the $m$=1 beams. The other key point in achieving these resolutions is the precise technology behind mask fabrication. Due to the short EUV wavelength, smallest defects and roughness of the gratings lead to incoherent scattering and deteriorate the aerial image quality. Our IL masks consist of Inpria IB gratings written by EBL and gold photonstops, all made on a 100-nm-thick $Si_3N_4$ membrane (Fig. 3). The underlying thin Cr layer between the membrane and the gratings, served as adhesion promoter, and was later dry etched in order to increase the diffraction efficiency. Using EBL, well-resolved and smooth lines of ≈14 nm wide ($P_g$=28 nm) could be achieved on the mask, which gives HP=7 nm structures on wafer (Fig. S1 in supplementary information). Patterns with smaller $P_g$s showed higher roughness and pattern collapse. Unlike common high-resolution masks made of HSQ gratings[33], the advantage of using gratings made of the Inpria resist here, is its higher EUV absorption (Fig. 2), which significantly increases the diffraction efficiency of the gratings on mask and therefore reduces the exposure times, resulting in minimized artefacts such as drifts and unexpected vibrations that may happen during the exposure. This resist is also well resistant against reactive ion etching (RIE) with Cl-containing recipes and the patterns were transferred into the underlying Cr layer (Fig. S1 in supplementary information). The mask efficiency is determined by the thickness, duty cycle, and the pitch of the gratings, which consists of resist and Cr layers, as well as the transmission of the support membrane. We used the rigorous coupled-wave analysis (RCWA) method[34, 35] in order to characterize the diffraction efficiency of the gratings for EUV light. Details of this characterization are listed in the supplementary information and we estimate the diffraction efficiency to be ≈2%, which is a good value for grating pitch of down to 28 nm and made possible by the use of Inpria IB which serves not only as a sensitive photoresist, but also as an effective optical element for EUV light.

The third technological advancement in achieving such a high resolution was the quality of the beam and the stability of the mechanical components. The exposures were done at the XIL-II beamline of Swiss Light Source, where over time the infrastructure and the instrumentation have evolved for making finer structures[36]. The EUV beam on the mask is spatially coherent and has relatively high flux of 35 mW/cm$^2$. It has a bandwidth of $\Delta\lambda/\lambda$=4% and this relatively high bandwidth has no impact on the aerial image according to Eq. 1. At such high resolutions vibrations and mechanical drifts of any kind easily deteriorate the aerial image and wash out the patterns. We note that the exposures can take above 100 s and extreme care and control of relative mask-to-wafer position are needed. As mentioned earlier, axial vibrations and drifts are not relevant due to the intrinsic independence of the aerial image to the axial distance of the mask to the wafer (Eq. 1).

Besides making line-space nanostructures using two-beam EUV-IL, we also patterned dot and hole arrays, which are also essential structures in semiconductor devices such as contact holes. Fig. 4 illustrates these structures made by appropriate arrangement of three- and four-beam gratings. While the one-dimensional lines were realized down to HP=7 nm, these two-dimensional structures were achieved down to HP=11 nm. We believe that the main reason for the better resolution in case of 1D structures than in 2D structures is due to the different demagnification of IL for different number of beams. Eq. 1 defines the HP for two-beam IL and shows that the printed lines



 

are a factor 2 denser than that in the mask grating for 1st order diffraction. In case of 3 and 4-beam IL, the corresponding demagnification factors are √3 and √2, respectively[24]. Since we are limited by the grating fabrication, the ultimate resolution for different IL configurations also differs. IL could also be used for making quasi-periodic nanostructures by using more complicated grating arrangements on the masks[25]. In order to pattern non-symmetric and ultimately functional circuits, IL could no longer be used and projection lithography will be needed.

Aside from exploring the capability of reaching single-digit patterning resolution, we also evaluated the capability of our resist in serving as a hard mask for pattern transfer. Fig. 5 illustrates etching 40 nm into Si, using an optimized RIE recipe, and making Si nanowires with HP=15 and 11 nm. In both cases Inpria IB patterns were used as hard masks and the linewidths down to 7 nm are obtained, which leads to an aspect ratio of ≈5.7. The photoresist was afterwards removed with a HF-buffer solution. For smaller HP values the Si etching process needs further optimization. Using HSQ as a hard mask was not effective for etching due to the poor RIE selectivity. There are currently significant efforts in developing RIE recipes and instrumentations that allow more anisotropic and selective etching processes[37, 38]. We hope that in the future these systems could be used for etching into denser lines.

## Discussion

The ultimate resolution limit of IL is $R=\lambda/4$, where for the $m=1$ interfering beams happens at $P_g=\lambda$. At this dimension the gratings only attenuate the incident beam and no longer diffract.

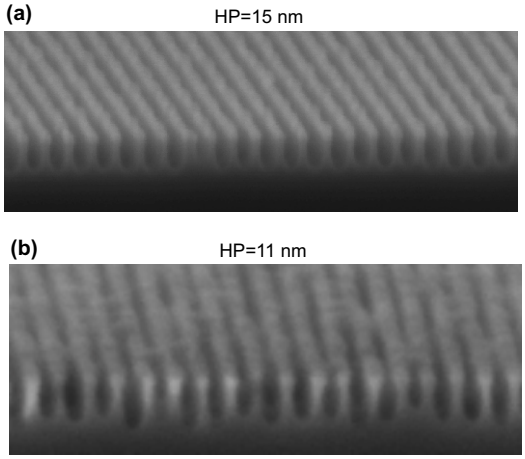


**Fig. 5** Pattern transfer into Si. Bird-eye view SEMs of Si line-space patterns with half-pitch values of (a) 15 nm and (b) 11 nm. These structures are 7 nm wide and 40 nm tall.

In the case of using EUV light this limit corresponds to $R\approx3.5$ nm, which is two times smaller than the HPs that we have achieved in the present study. In reaching the capability of making such dense structures the major challenges is pattern collapse on wafer. Even though the HSQ is known to be mechanically stable and the height of the structures were ≈20 nm, when HP<10 nm, the resist adhesion and pattern collapse become challenging. Further reduction of resists thickness leads to non-uniformity in its thickness and increase in the LER. As mentioned earlier patterning structures denser than $P_g=28$ nm using EBL is another challenge due to the secondary electron blur. This effect might be circumvented by making narrower lines with duty cycles < 0.5, that in turn results in lower diffraction efficiency and higher chances of pattern collapse. We therefore foresee making denser structures by using methods that reduce this effect such as supercritical drying. Inspired by advances in X-ray diffraction optics[39], the grating frequency could also be doubled by atomic layer deposition techniques. In addition, IL could be adopted for making twice denser patterns by interfering the second-order diffracted beam ($m=2$)[27], which in turn increases the requirements for stage stability due to the relatively low diffraction efficiency and thereby relatively long exposure times.

Our successful establishment of an EUV-IL system for making dense lines with HP=7 nm, proves the capability of photolithography in reaching single-digit technology nodes. In modern IC manufacturing, a technology node value is smaller than the fabrication HP, and in the case of CMOS logic devices, for example, is a parameter closer to the physical gate length[40]. According to the ITRS, 2D Flash devices with minimum feature sizes of HP=8 nm would satisfy the specs of the 2.5 nm technology node and beyond, which is expected to be reached in 2023. For the Logic and DRAM devices, nevertheless, making structures with HP<10 nm resolution addresses even technology nodes subsequent to the 1.8 nm node and is perceived to be achieved several years later[23]. Demonstrating the capability of using EUV light for patterning 2D and 1D arrays (Figs 1 and 4) with cutting edge resolutions proves the feasibility of using EUVL for reaching the 2.5 nm technology node and beyond. Moreover, the fact that the HfO-based photoresist, Inpria IB, provides high-resolution periodic patterns with HP=8 nm and smooth edges, and that it is a relatively sensitive EUV resist indicates reaching a milestone in the Si semiconductor industry. Indeed, further development of more sensitive photoresist chemistries will facilitate bringing these technology nodes into HVM. It is clear, however, that many other technologies besides the photochemistry development should advance in parallel for reaching such goals and hence functional devices. These include light source, overlay accuracy, defects at the mask and wafer levels, to name a few.

## Conclusions

The structures we fabricated were etch resistance and were used to transfer the line-space patterns into Si with HP=11 nm and aspect ratio of ≈5.7. The tendency of using inorganic photoresists in efficient EUVL can also be seen in other studies[30, 41, 42]. It seems that adopting these chemistries to elements that have higher EUV absorption could increase the sensitivity and potentially meeting RLS requirements of the industry and being used for HVM. Our results verify IL being a

robust tool for minimizing imaging artefacts at EUV and using it for the exploration of EUV photoresists. We foresee the improvement of different aspects of EUV-IL in the near future in order to continue towards the ultimate resolution of photolithography at 13.5 nm wavelength. These improvements would also assist exploring patterning at even shorter wavelengths of 6.x nm, for reaching higher resolutions[1, 2, 43]. Sub-10 nm half-pitch range is a very exciting regime in terms of physics, where quantum effects and single electron mechanisms start to play a dominant role. This regime has been the domain of bottom-up approaches, such as chemical synthesis, and top-down and generic nanofabrication methods will enable better control and increased complexity. Pattern transfer into functional nanostructures in this range remains a significant challenge and is the subject of future studies.

## Acknowledgements

We would like to thank Michaela Vockenhuber and Markus Kropf for technical support, Sangsul Lee and Jason Stowers for fruitful discussions, and Inpria Corp. for providing photoresists. Part of this work was carried out at the Swiss Light Source, Paul Scherrer Institute.

## Notes

[a] Laboratory for Micro- and Nanotechnology, Paul Scherrer Institute, 5232 Villigen, Switzerland.

[b] Roche Diagnostics International Ltd. Forrenstrasse, 6343 Rotkreuz, Switzerland.

[c] Eulitha, Industristrasse Althau 1, 5303 Wurelingen, Switzerland.

* E-mail: nassir-mojarad@ethz.ch; Present address: Nanotechnology Group, ETH Zurich, Säumerstrasse 4, 8803 Rüschlikon, Switzerland; Fax: +41446321278; Tel: +41446326642. E-mail: yasin.ekinci@psi.ch; Fax: +41563102646; Tel: +41563102824.

† Electronic Supplementary Information (ESI) available: Mask fabrication. Diffraction efficiency simulations. Critical dimension (CD) as a function of dose for Inpria XE15IB (IB). EUV lithography and photoresist preparation. Reactive-ion etching. See DOI: 10.1039/b000000x/

†† These authors contributed equally to this work.

## References

1. G. Tallents, E. Wagenaars and G. Pert, *Nature Photonics*, 2010, 4, 809-811.
2. C. Wagner and N. Harned, *Nature Photonics*, 2010, 4, 24-26.
3. R. Peeters, S. Lok, E. van Alphen, N. Harned, P. Kuerz, M. Lowisch, H. Meijer, D. Ockwell, E. van Setten and G. Schiffelers, *SPIE Advanced Lithography*, 2013, 8679, 86791F.
4. C. G. Willson and B. J. Roman, *ACS Nano*, 2008, 2, 1323-1328.
5. D. T. Attwood, *Soft X-Rays and Extreme Ultraviolet Radiation: Principles and Applications*, Cambridge University Press, 2000.
6. M. D. Austin, W. Zhang, H. X. Ge, D. Wasserman, S. A. Lyon and S. Y. Chou, *Nanotechnology*, 2005, 16, 1058-1061.
7. M. D. Fischbein and M. Drndic, *Nano Letters*, 2007, 7, 1329-1337.
8. Z. S. Gan, Y. Y. Cao, R. A. Evans and M. Gu, *Nature Communications*, 2013, 4, 2061.
9. F. W. Huo, G. F. Zheng, X. Liao, L. R. Giam, J. A. Chai, X. D. Chen, W. Y. Shim and C. A. Mirkin, *Nature Nanotechnology*, 2010, 5, 637-640.
10. V. R. Manfrinato, L. H. Zhang, D. Su, H. G. Duan, R. G. Hobbs, E. A. Stach and K. K. Berggren, *Nano Letters*, 2013, 13, 1555-1558.
11. R. V. Martinez, N. S. Losilla, J. Martinez, Y. Huttel and R. Garcia, *Nano Letters*, 2007, 7, 1846-1850.
12. D. Pires, J. L. Hedrick, A. De Silva, J. Frommer, B. Gotsmann, H. Wolf, M. Despont, U. Duerig and A. W. Knoll, *Science*, 2010, 328, 732-735.
13. R. G. Hobbs, N. Petkov and J. D. Holmes, *Chemistry of Materials*, 2012, 24, 1975-1991.
14. H. S. Lee, B. S. Kim, H. M. Kim, J. S. Wi, S. W. Nam, K. B. Jin, Y. Arai and K. B. Kim, *Advanced Materials*, 2007, 19, 4189-4193.
15. L. Pain, S. Tedesco and C. Constancias, *Comptes Rendus Physique*, 2006, 7, 910-923.
16. T. Chang, M. Mankos, K. Y. Lee and L. P. Muray, *Microelectronic Engineering*, 2001, 57, 117-135.
17. E. A. Costner, M. W. Lin, W.-L. Jen and C. G. Willson, *Annual Review of Materials Research*, 2009, 39, 155-180.
18. W. Zhou, *Nanoimprint Lithography: An Enabling Process for Nanofabrication*, Springer, 2013.
19. C. Reboul, G. Fleury, K. Aissou, C. Brochon, E. Cloutet, C. Nicolet, X. Chevalier, C. Navarro, R. Tiron and G. Cunge, *SPIE Advanced Lithography*, 2014, 9049, 904925.
20. M. P. Stoykovich and P. F. Nealey, *Materials Today*, 2006, 9, 20-29.
21. H. Tsai, J. W. Pitera, H. Miyazoe, S. Bangsaruntip, S. U. Engelmann, C.-C. Liu, J. Y. Cheng, J. J. Bucchignano, D. P. Klaus and E. A. Joseph, *ACS Nano*, 2014, 8, 5227-5232.
22. H. J. Levinson, *Principles of Lithography*, SPIE Press, 2011.
23. http://www.itrs.net/Links/2013ITRS/Home2013.htm.
24. B. Terhalle, A. Langner, B. Paivanranta and Y. Ekinci, *Proc. SPIE*, 2011, 8102, 81020V.
25. A. Langner, B. Paivanranta, B. Terhalle and Y. Ekinci, *Nanotechnology*, 2012, 23.
26. Y. Ekinci, M. Vockenhuber, M. Hojeij, L. Wang and N. M. Mojarad, *SPIE Advanced Lithography*, 2013, 8679, 867910.
27. B. Paivanranta, A. Langner, E. Kirk, C. David and Y. Ekinci, *Nanotechnology*, 2011, 22.
28. A. Grigorescu and C. Hagen, *Nanotechnology*, 2009, 20, 292001.
29. D. L. Olynick, B. Cord, A. Schipotinin, D. F. Ogletree and P. J. Schuck, *Journal of Vacuum Science & Technology B*, 2010, 28, 581-587.
30. R. P. Oleksak, R. E. Ruther, F. Luo, K. C. Fairley, S. R. Decker, W. F. Stickle, D. W. Johnson, E. L. Garfunkel, G. S. Herman and D. A. Keszler, *ACS Applied Materials & Interfaces*, 2014, 6, 2917-2921.
31. R. E. Ruther, B. M. Baker, J. H. Son, W. H. Casey and M. Nyman, *Inorganic Chemistry*, 2014, 53, 4234-4242.
32. http://henke.lbl.gov/optical_constants/.
33. N. Mojarad, D. Fan, J. Gobrecht and Y. Ekinci, *Optics Letters*, 2014, 39, 2286-2289.
34. http://photonics.intec.ugent.be/research/facilities/design/rodis/.
35. M. G. Moharam and T. K. Gaylord, *Journal of the Optical Society of America*, 1981, 71, 811-818.
36. Y. Ekinci, M. Vockenhuber, N. Mojarad and D. Fan, *SPIE Advanced Lithography*, 2014, 9048, 904804.
37. E. A. Joseph, S. U. Engelmann, H. Miyazoe, R. L. Bruce, M. Nakamura, T. Suzuki and M. Hoinkis, *Proc. SPIE*, 2013, 8685, 86850A.
38. Z. Liu, Y. Wu, B. Harteneck and D. Olynick, *Nanotechnology*, 2013, 24, 015305.
39. K. Jefimovs, J. Vila-Comamala, T. Pilvi, J. Raabe, M. Ritala and C. David, *Physical Review Letters*, 2007, 99.
40. H. Iwai, *Microelectronic Engineering*, 2009, 86, 1520-1528.
41. W. J. Bae, M. Trikeriotis, J. Sha, E. L. Schwartz, R. Rodriguez, P. Zimmerman, E. P. Giannelis and C. K. Ober, *Journal of Materials Chemistry*, 2010, 20, 5186-5189.
42. J. Stowers and D. A. Keszler, *Microelectronic Engineering*, 2009, 86, 730-733.
43. N. Mojarad, M. Vockenhuber, L. Wang, B. Terhalle and Y. Ekinci, *SPIE Advanced Lithography*, 2013, 8679, 867924.



 